

Fine-scale structure of the San Andreas fault zone and location of the SAFOD target earthquakes

C. Thurber,¹ S. Roecker,² H. Zhang,¹ S. Baher,^{1,3} and W. Ellsworth⁴

Received 31 December 2003; revised 2 February 2004; accepted 17 February 2004; published 18 May 2004.

[1] We present results from the tomographic analysis of seismic data from the Parkfield area using three different inversion codes. The models provide a consistent view of the complex velocity structure in the vicinity of the San Andreas, including a sharp velocity contrast across the fault. We use the inversion results to assess our confidence in the absolute location accuracy of a potential target earthquake. We derive two types of accuracy estimates, one based on a consideration of the location differences from the three inversion methods, and the other based on the absolute location accuracy of “virtual earthquakes.” Location differences are on the order of 100–200 m horizontally and up to 500 m vertically. Bounds on the absolute location errors based on the “virtual earthquake” relocations are ~50 m horizontally and vertically. The average of our locations places the target event epicenter within about 100 m of the SAF surface trace. *INDEX TERMS:* 7203 Seismology: Body wave propagation; 7205 Seismology: Continental crust (1242); 7215 Seismology: Earthquake parameters; 8015 Structural Geology: Local crustal structure; 8180 Tectonophysics: Tomography. **Citation:** Thurber, C., S. Roecker, H. Zhang, S. Baher, and W. Ellsworth (2004), Fine-scale structure of the San Andreas fault zone and location of the SAFOD target earthquakes, *Geophys. Res. Lett.*, 31, L12S02, doi:10.1029/2003GL019398.

1. Introduction

[2] One of the many exciting scientific components of the San Andreas Fault Observatory at Depth (SAFOD) project is the opportunity to drill into the rupture patch of a magnitude ~2 earthquake [Ellsworth *et al.*, 2000] (Figure 1). This opportunity presents an enormous challenge, though, first requiring targeting of the main SAFOD borehole close enough to the rupture patch for a subsequent satellite corehole to reach it (~100 m), and then requiring knowledge of the target hypocenter to an absolute accuracy of about 10 m to allow intelligent targeting of the satellite corehole. Relative location techniques capitalizing on waveform alignment methods have achieved this level of relative location accuracy [e.g., Rubin *et al.*, 1999; Waldhauser and Ellsworth, 2000, 2002; Rowe *et al.*, 2002], but the same claim cannot be made for absolute location accuracy.

¹Department of Geology and Geophysics, University of Wisconsin-Madison, Madison, Wisconsin, USA.

²Department of Earth and Environmental Sciences, Rensselaer Polytechnic Institute, Troy, New York, USA.

³Now at U.S. Geological Survey, Menlo Park, California, USA.

⁴U.S. Geological Survey, Menlo Park, California, USA.

[3] We present the results from the tomographic analysis of earthquake and explosion arrival time data from the Parkfield area, using three different inversion codes. The models provide a consistent view of the complex crustal structure in the vicinity of the San Andreas fault (SAF) in Parkfield. We also use these inversions to explore and assess our confidence in the absolute location accuracy of a potential SAFOD target earthquake that occurred in March 2001. This work improves upon the preliminary results of Thurber *et al.* [2003] by incorporating data from the borehole seismic string deployed in the SAFOD Pilot Hole in July 2002 and from shots detonated in October 2002, as well as including data from nearly twice as many earthquakes. We also derive two types of accuracy estimates, one based on a consideration of the location differences from the three inversion methods and the other based on the absolute location accuracy of “virtual earthquakes” (shot data from SAFOD Pilot Hole receiver gathers treated as if they were earthquakes). We conclude that further improvement in the location accuracy is required to help in targeting the initial phases of SAFOD drilling. Fortunately, new active-source data collected in November 2003 should provide enough new constraints to reach the initial accuracy goals.

2. Dataset and Tomographic Inversion Methods

[4] The temporary seismic array “PASO” (Parkfield Area Seismic Observatory) was installed around Parkfield, CA, beginning in July 2000 (Figure 2). Initially, 15 3-component recording instruments were deployed from the Program for the Array Seismic Studies of the Continental Lithosphere (PASSCAL) of the Incorporated Research Institutions for Seismology (IRIS). In July of 2001, 44 additional PASSCAL 3-component stations were deployed within the aperture of the original array, and 2 of the original stations were moved. The entire array was removed in late October 2002, following the detonation of a set of “calibration” shots (Figure 2).

[5] Nearly 90,000 arrival times (65% P, 35% S) from over 800 local earthquakes and about 100 explosions were included in joint inversions for earthquake locations and 3D Vp and Vp/Vs structure. The data were obtained from PASO, the UC-Berkeley High Resolution Seismic Network (HRSN), field projects in 1994 [Li *et al.*, 1997] and 1998 [Hole *et al.*, 2001; Catchings *et al.*, 2002], and from the USGS Central California Seismic Network. The sample rates for the PASO and the USGS stations are 100 sps, whereas it is 250 sps for the HRSN.

[6] The arrival time data were inverted using 3 different tomography codes. The code simul2000 [Thurber and Eberhart-Phillips, 1999] was used to determine a 3D model with mostly kilometer-scale gridding, and also a “focused”

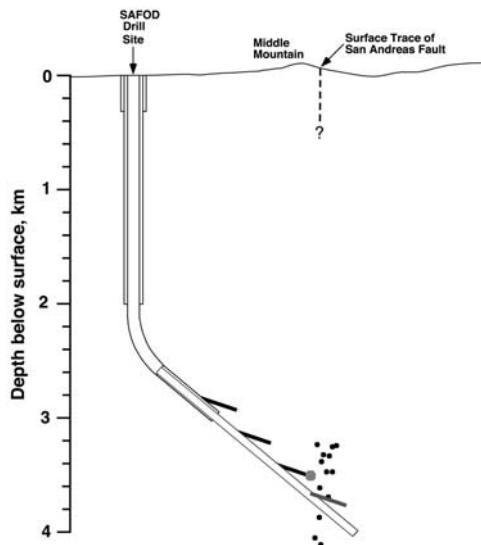


Figure 1. Cartoon illustrating the SAFOD drilling plan and the targeting of a magnitude 2 earthquake rupture patch.

2D model with 500 m grid spacing near the fault. The double-difference tomography code *tomoDD* [Zhang and Thurber, 2003] was also used to derive a kilometer-scale model. Initial models for these inversions included a modest (~ 0.6 km/s) across-fault velocity contrast. Finally, the code *tomoGRAV* [Roecker *et al.*, 2004] was used to model the structure with as fine as 200 m gridding, using a one-dimensional starting model. As the name implies, *tomoGRAV* jointly fits arrival time data and gravity residuals using a local velocity-density relationship. The gravity data [McPhee and Jachens, 2004], which were obtained at much more closely spaced points than our seismic stations, provide valuable constraints where the seismic data are sparse, especially in the near surface between seismic station sites. For additional details on the joint seismic-gravity inversion, the reader is referred to Roecker *et al.* [2004].

[7] Figure 3 compares cross-sections normal to the SAF through the Pilot Hole for the 3D *simul2000* and *tomoDD* models. For examples of how the structure varies along strike of the fault, the reader is referred to Thurber *et al.* [2003]. The earthquake locations are more tightly clustered in the *tomoDD* result on the right, as expected. Otherwise, the model results are quite comparable. The fault zone is marked by a sharp horizontal velocity gradient that steps several hundred meters northeastward at about 2 km below sea level, which is the depth at which seismicity begins. Note that below 5 km depth, we are losing resolution. To the northeast of the fault zone, we find a relatively low velocity region extending to a depth of about 4 km. Southwest of the fault zone, there is a high velocity body adjacent to the area of seismicity. These main features are prevalent in other cross-sections and in our other models.

[8] Figure 4 shows two different attempts to push towards higher spatial resolution in our modeling. On the left is a 2D model obtained with *simul2000*. Here, data from sources and receivers only within a bow-tie-shaped region centered on the SAF trace (indicated in Figure 2) were

included in the inversion. On the right is a slice through the 3D model from the joint seismic-gravity inversion. The model features are generally similar to each other and to the two preceding models, but there are some noteworthy differences in the *tomoGRAV* model. Southwest of the fault, there is a velocity reversal at depths ranging from 3 to 5 km. Beneath the fault, the lateral velocity gradient is more evident to a greater depth. Northeast of the fault, the low velocity region extends to a significantly greater depth.

[9] It is illuminating to compare the main features of the seismic results to the resistivity models of Unsworth *et al.* [2000] and Unsworth and Bedrosian [2004] for the same section. The seismic and MT models bear a strong similarity. Inferred basement depth differences on the two sides of the fault are comparable. The high velocity body southwest of the fault matches the highly resistive body in the MT model. The very low resistivity region at shallow depths between the Pilot Hole and the SAF aligns with the low velocity region adjacent to the fault, a zone inferred to be fluid-rich. Finally, the low velocity region northeast of the fault corresponds quite well with the northeastern low resistivity zone in the MT model (referred to as the Eastern Conductor) [Unsworth and Bedrosian, 2004], also inferred to be fluid-rich.

3. Target Earthquake Location Uncertainty Estimates

[10] For the purposes of SAFOD, the most important information we need to provide is the location of the target

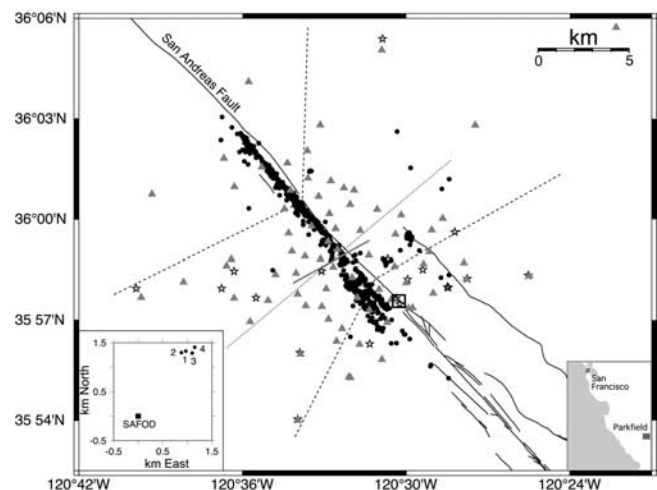


Figure 2. Map view of the PASO array and permanent network stations along the SAF near Parkfield. Lower right inset indicates the area of study. Fault traces are indicated by black lines, the approximate 1966 Parkfield epicenter is indicated by the open square, triangles are PASO, USGS, and HRSN stations, the gray line indicates the PSINE profile [Catchings *et al.*, 2002], the dotted line indicates the cross-section for the models presented in Figures 3 and 4, and the large shots are indicated by stars. The dashed lines enclose the stations and sources included in the 2D inversion (all were included in the 3D inversion). Lower left inset: comparison of four estimates of the target event epicenter (see Table 1).

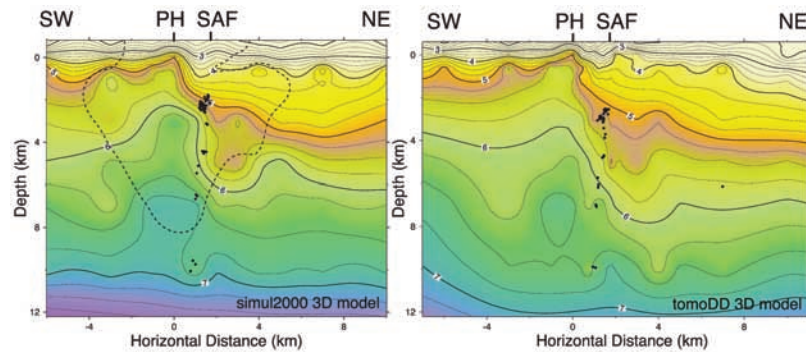


Figure 3. Comparison of cross-sections through the SAFOD Pilot Hole from the simul2000 (left) and tomoDD (right) 3D models. Earthquakes within 1 km of the section are shown (filled circles), and the positions of the Pilot Hole (PH) and SAF trace (SAF) are indicated. Depths are relative to sea level. The 0.2 contour of the diagonal element of the model resolution matrix is shown in the simul2000 result (dashed line). Resolution in the other solutions is equivalent or better.

magnitude 2 earthquake. Table 1 lists the location estimates from the four solutions relative to the location of the SAFOD Pilot Hole; the epicenters are shown in the inset in Figure 2. The average of the four estimates places the earthquake about 1 km E and 1.3 km N of the Pilot Hole, at a little less than 3 km below the surface. The RMS scatter in these locations is about 100 m horizontally and 180 m vertically. Linear and fully nonlinear estimates of the location uncertainty for the individual locations are of a similar size.

[11] Unfortunately, these estimates only provide relative location uncertainties. In order to provide an absolute error estimate, we make use of the “virtual earthquakes.” Using arrival times measured at each borehole geophone for all of the October 2002 shots, we assemble a “receiver gather” of all the shots observed at a given geophone and treat the data as if it came from an “earthquake” in the Pilot Hole recorded at “stations” located at the shot points (our “virtual earthquake”). When we locate these “virtual earthquakes” in our models, the absolute location errors are on the order of 50 m horizontally and vertically. The deepest “virtual earthquakes” are less than 2 km away from the target earthquake region, so this provides us with confidence that our absolute locations are of high quality. We also locate each of the October 2002 shots individually,

treating them as earthquakes. Location errors for shots close to the center of the array are on the order of 100 m or less horizontally and vertically, whereas for the shots around the perimeter of the array, location errors are about a factor of two larger.

4. Discussion and Conclusions

[12] The average of our target event locations places its epicenter within about 100 m of the SAF surface trace, about 1.7 km NNE of the SAFOD site. Location differences from the four tomography solutions are on the order of 100–200 m horizontally and up to 500 m vertically, probably due to differences in model gridding, travel time calculation method, and solution regularization. Thus we have not yet reached the necessary ~ 100 m accuracy level. In contrast, typical absolute location errors based on the “virtual earthquake” relocations are ~ 50 m horizontally and vertically. This suggests that our location accuracy goal can be reached, in principle.

[13] What can be done to improve our locations? In November 2003, a major active-source experiment was carried out around Parkfield. These new data will provide strong constraints on our velocity models, and should help reduce the disagreements among the different models. We

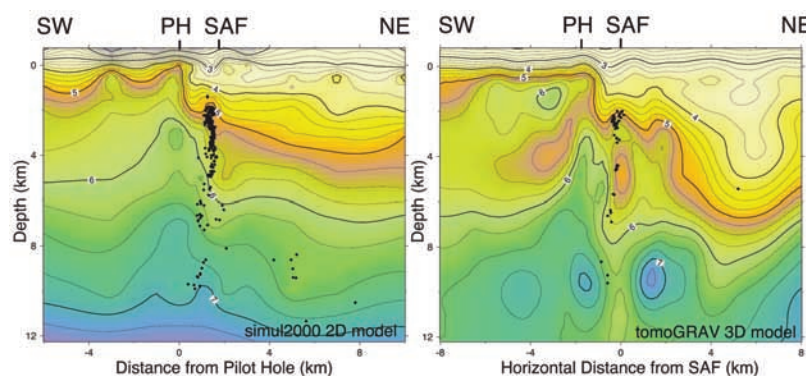


Figure 4. Comparison of cross-sections through the SAFOD Pilot Hole from the simul2000 2D model (left) and tomoGRAV 3D model (right). Note that there are many more earthquakes on the 2D simul2000 model, as all events included in the inversion are projected onto the section. The positions of the Pilot Hole (PH) and SAF trace (SAF) are indicated. Depths are relative to sea level.

Table 1. Comparison of Locations of the Target Earthquake From the Four Tomography Solutions

Location Method	Km E of SAFOD	Km N of SAFOD	Depth ^a	Depth BSL
1. 3D simul2000	0.97	1.33	2.73	2.00
2. 2D simul2000	0.88	1.30	2.81	2.08
3. tomoDD	1.10	1.29	3.22	2.51
4. tomoGRAV	1.15	1.41	2.78	2.05
AVERAGE	1.02	1.33	2.88	2.16

^arelative to the surface at the epicenter.

will also have another critical opportunity to refine and assess our models and locations after Phase 1 of SAFOD drilling is completed. The drilling will be halted while the borehole is still in relatively intact bedrock outside the fault zone, at which point a borehole geophone will be installed at the bottom of the hole for approximately one year of monitoring. A number of small shots will be carried out, giving us an additional “virtual earthquake” that will be only about a kilometer from the target region, helping us to refine further the accuracy of our target event location.

[14] **Acknowledgments.** We thank Leonard Johnson for support and for facilitating a timely start to this project, and we thank the landowners of the Parkfield area for providing access to their land and for their cooperation during our long-term deployment. We especially want to thank Lee Powell, Bill Unger, Glen Offield, Steve Hickman, Tom Burdette, Gary Fuis, and Michael Rymer for their assistance. We also acknowledge Gary Fuis and Ron Kaderabek for their work loading shots, and Gray Jensen, Jim Luetgert, Dave Croker, Dave Reneau, and Tom Burdette for their work doing the shooting. We thank Doug Neuhauser and the Northern California Earthquake Data Center for access to data from the Northern California Seismic Network of the U.S. Geological Survey, Menlo Park, and the High Resolution Seismic Network of the Berkeley Seismological Laboratory, University of California, Berkeley. We are also extremely grateful to the many other PASSCAL, IRIS Data Management System, UW-Madison, RPI, UC-San Diego, UC-Berkeley, and USGS staff and students who played a role in the success of this project. This research was supported by the Continental Dynamics program of NSF, under grants EAR-9814192 (UW) and EAR-9814155 (RPI). The instruments used in the field program were provided by the PASSCAL facility of the Incorporated Research Institutions for Seismology (IRIS) through the PASSCAL Instrument Center at New Mexico Tech. Data collected during this experiment will be available through the IRIS Data Management Center. The facilities of the IRIS Consortium are supported by the National Science Foundation under Cooperative Agreement EAR-0004370.

References

Catchings, R. D., M. J. Rymer, M. R. Goldman, J. A. Hole, R. Huggins, and C. Lippus (2002), High-resolution seismic velocities and shallow struc-

ture of the San Andreas fault zone at Middle Mountain, Parkfield, California, *Bull. Seismol. Soc. Am.*, *92*, 2493–2503.

Ellsworth, W. L., S. H. Hickman, and M. D. Zoback (2000), Seismology in the source: The San Andreas Fault Observatory at Depth (SAFOD) (abstract), *Seismol. Res. Lett.*, *71*, 252.

Hole, J. A., R. D. Catchings, K. C. St. Clair, M. J. Rymer, D. A. Okaya, and B. J. Carney (2001), Steep-dip imaging of the shallow San Andreas fault near Parkfield, *Science*, *294*, 1513–1515.

Li, Y.-G., W. L. Ellsworth, C. H. Thurber, P. Malin, and K. Aki (1997), Fault-zone guided waves from explosions in the San Andreas fault at Parkfield and Cienega Valley, California, *Bull. Seismol. Soc. Am.*, *87*, 210–221.

McPhee, D., R. C. Jachens, and C. M. Wentworth (2004), Crustal structure across the San Andreas fault at the SAFOD site from potential field and geologic studies, *Geophys. Res. Lett.*, *31*, L12S03, doi:10.1029/2003GL019363.

Roecker, S., C. Thurber, and D. McPhee (2004), Joint inversion of gravity and arrival time data from Parkfield: New constraints on structure and hypocenter locations near the SAFOD drill site, *Geophys. Res. Lett.*, *31*, L12S04, doi:10.1029/2003GL019396.

Rowe, C. A., R. C. Aster, W. S. Phillips, R. H. Jones, B. Borchers, and M. C. Fehler (2002), Relocation of induced microearthquakes at the Soultz geothermal reservoir using automated, high-precision picking, *Pure Appl. Geophys.*, *159*, 563–596.

Rubin, A. M., D. Gillard, and J.-L. Got (1999), Streaks of microearthquakes along creeping faults, *Nature*, *400*, 635–641.

Thurber, C., and D. Eberhart-Phillips (1999), Local earthquake tomography with flexible gridding, *Comput. Geosci.*, *25*, 809–818.

Thurber, C., S. Roecker, K. Roberts, M. Gold, L. Powell, and K. Ritterger (2003), Earthquake locations and three-dimensional fault zone structure along the creeping section of the San Andreas Fault near Parkfield, CA: Preparing for SAFOD, *Geophys. Res. Lett.*, *30*(3), 1112, doi:10.1029/2002GL016004.

Unsworth, M., and P. Bedrosian (2004), Electrical resistivity at the SAFOD site from magnetotelluric exploration, *Geophys. Res. Lett.*, *31*, L12S05, doi:10.1029/2003GL019405.

Unsworth, M., P. Bedrosian, M. Eisel, G. Egbert, and W. Siripunvaraporn (2000), Along strike variations in the electrical structure of the San Andreas fault at Parkfield, California, *Geophys. Res. Lett.*, *27*, 3021–3024.

Waldhauser, F., and W. L. Ellsworth (2000), A double-difference earthquake location algorithm: Method and application to the northern Hayward Fault, *CA, Bull. Seismol. Soc. Am.*, *90*, 1353–1368.

Waldhauser, F., and W. L. Ellsworth (2002), Fault structure and mechanics of the Hayward Fault, California, from double-difference earthquake locations, *J. Geophys. Res.*, *107*(B3), 2054, doi:10.1029/2000JB000084.

Zhang, H., and C. H. Thurber (2003), Double-difference tomography: The method and its application to the Hayward fault, California, *Bull. Seismol. Soc. Am.*, *93*, 1875–1889.

S. Baher and W. Ellsworth, U.S. Geological Survey, 345 Middlefield Rd., Menlo Park, CA 94035, USA.

S. Roecker, Department of Earth and Environmental Sciences, Rensselaer Polytechnic Institute, Troy, NY 12180, USA.

C. Thurber and H. Zhang, Department of Geology and Geophysics, University of Wisconsin-Madison, 1215 W. Dayton St., Madison, WI 53706, USA. (thurber@geology.wisc.edu)